Paper No.
6113

NACE INTERNATIONAL CORROSION 2015 CONFERENCE & EXPO

Flow Patterns and Water Wetting in Gas-Oil-Water Three-phase Flow – A Flow Loop Study

Kok Eng Kee*, Marijan Babic, Sonja Richter, Luciano Paolinelli, Wei Li, Srdjan Nesic
Institute for Corrosion and Multiphase Technology
Ohio University, Athens, OH 45701
*Universiti Teknologi Petronas, Malaysia

ABSTRACT

In the oil and gas industry, multiphase flow environments are frequently encountered during the production and transportation of hydrocarbon products *via* pipelines. Most oil production wells naturally contain some fraction of water and gases. These fluids often flow concurrently in the pipelines, leading to a variety of complex flow patterns. However, the presence of acid gases such as CO_2 and H_2S soluble in the water can lead to internal corrosion attack if the water comes into contact with the mild steel pipe wall, a scenario known as 'water wetting'.

In this experimental work, a large-scale 0.1 m ID inclinable flow loop was used to study the three-phase gas-oil-water flow in horizontal and vertical positions. A light model oil (ρ_o = 823 kg/m^3, μ_o = 2.7 cP), an aqueous 1 wt.% NaCl solution and CO_2 gas were utilized as the test fluids. Two measurement techniques: high speed video camera and flush mounted conductivity pins were employed for flow pattern visualization and surface wetting measurements, respectively. The flow patterns and surface wetting behaviors were quantified at various liquid velocities, gas velocities and water cuts up to 20%. The flow patterns were classified according to the global gas-liquid structure and local oil-water distribution. The flow patterns were seen to change from stratified to intermittent and finally annular-mist flows as the superficial gas velocity increased, while the local oil and water phases were either separated or dispersed. At low water cut, the wetting results showed that adding the gas phase can help to keep water away from the pipe wall, leading to oil wetting. At high water cut, water wetting prevailed and the flow of gas did not lessen the intensity of water wetting.

Keywords: water wetting, gas-oil-water flow, flow pattern, conductivity pin, wettability

INTRODUCTION

Much of the research work on water wetting has been directed to understand the wetting behavior in two-phase oil-water flow.[1-7] Researchers at Ohio University have successfully employed multi-array conductivity probes to study the water wetting behavior of oil-water flow in a large-scale flow loop.[4-7] There has been an extensive body of experimental work on the hydrodynamics and flow characteristics in two-phase (gas-liquid, oil-water) and three-phase (gas-oil-water) flow systems.[8-13] The work mostly focused on the flow patterns, pressure gradient, liquid holdup and other flow-pattern-specific hydrodynamic parameters. Little or no attention has been placed on the study of water wetting in three-phase flow. It is known that a wide variety of complex flow patterns can arise when moving two or more

immiscible phases simultaneously in pipes. If water is present in the multiphase pipe flow, corrosion can often pose a threat when free water comes in contact with the mild steel wall. Hence, it is of paramount importance to study the distribution of water in a three-phase flow environment since it is closely related to the water wetting phenomenon in the pipe.

In gas-oil-water flow, the major flow structures are dictated more prominently by the spatial distribution of the gas and the liquid phases and to a lesser extent by the oil and the water phases distribution within the liquid, due to the large contrast in physical properties between the gas and liquid phases. Hence in this work, the gas-oil-water flow patterns are primarily categorized according to the global flow structure seen in gas-liquid flow, and then refined by incorporating the local distribution of oil-water phases within a given gas-liquid flow pattern.[14] They are described and illustrated in Figure 1 for horizontal pipe orientation:

- *Stratified (ST)* flow is characterized by the concurrent flow of liquid streams at the bottom and a gas stream at the top of the pipe. The two liquid phases are often separated or slightly dispersed at the oil-water interface. The gas-liquid interface may be smooth or show some waviness caused by the drag of the gas passing over the liquid.
- *Elongated bubble (EB)* flow also called plug flow, is a form of intermittent flow that occurs at low gas velocity. It has the characteristic feature of long gas pockets trapped at the pipe top, moving alternately in between continuous sections of liquid that fully occupy the pipe. Water flows at the pipe bottom, mostly separated.
- *Slug (SL)* flow occurs when the liquid bridges the entire pipe cross section forming a liquid slug, whilst the gas flows as a large bubble in between the train of liquid slugs.[15] The large gas bubble moves on top of a slower moving stratified liquid layer characterized as the gas bubble-liquid film zone. The liquid slug, wetting the entire pipe section, moves more energetically and overruns the slow flowing liquid film ahead of it. The slug front is a highly turbulent liquid mixing region populated by small gas bubbles. The slugs contribute to large pressure fluctuation at each passage. The water is dispersed at the slug front, but becomes separated at the pipe bottom in the stratified zone.
- *Wavy annular (WA)* flow occurs at the transition between slug and annular flow. The flow lacks the characteristic pressure fluctuation found in slug flow. High amplitude waves are found to sweep momentarily around the pipe periphery but do not quite bridge the pipe top. The upper wall is occasionally wetted by an unstable liquid film that keeps falling diagonally downward.[16] The breakup of the unstable waves becomes a source for droplet entrainment in the gas phase. The water is usually dispersed, mostly distributed along the pipe circumference.
- *Annular-mist (AM)* flow occurs at very high gas velocity where gas flows at the pipe core and liquid moves as an annular film enveloping the pipe wall. The turbulent gas contributes to rough gas-liquid interfaces containing interfacial waves of varying amplitudes.[17] Some liquid droplets are entrained as mist in the gas core. The liquid film may be distributed thicker at the base than the top of pipe due to the gravity. The water is highly dispersed in the annular liquid film moving circumferentially along the pipe wall.

The general distribution and location of water in three-phase flow system is summarized in Table 1.

Table 1
Water distribution in gas-oil-water flow

No.	Flow patterns	Water distribution, location
1	Stratified (ST)	separated, bottom
2	Elongated bubble (EB)	separated, bottom
3	Slug (SL)	dispersed/separated, mostly bottom
4	Wavy annular (WA)	dispersed, mostly circumferential
5	Annular-mist (AM)	dispersed, circumferential

In the vertical gas-oil-water flow, two types of flow patterns can be observed under the current test conditions. They are described and illustrated in Figure 2:

- *Churn* is a form of intermittent flow where periodical flow reversal of liquid film is observed as an oscillatory liquid motion. The bulk liquid mass and gas chunks are greatly distorted in a chaotic fashion.[18] Water is mostly dispersed, found in the liquid film and the bulk liquid mass.
- *Annular–mist* occurs at very high gas velocities with gas flowing in the pipe core and thin liquid film flowing upward as an annulus around the pipe periphery. Disturbance waves at the film interface may occasionally break up as small entrained droplets (mist) in the central gaseous core. Water is dispersed in the annular liquid film enveloping the pipe circumference.

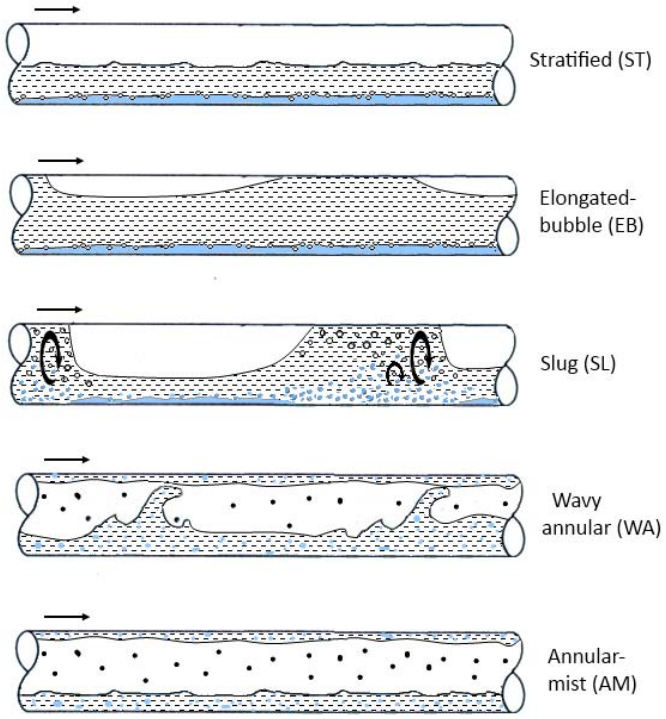

Figure 1: Schematics of oil-continuous horizontal three-phase flow patterns showing stratified, elongated bubble, slug, wavy annular and annular-mist flows. Images adapted from Shoham's text.[16]

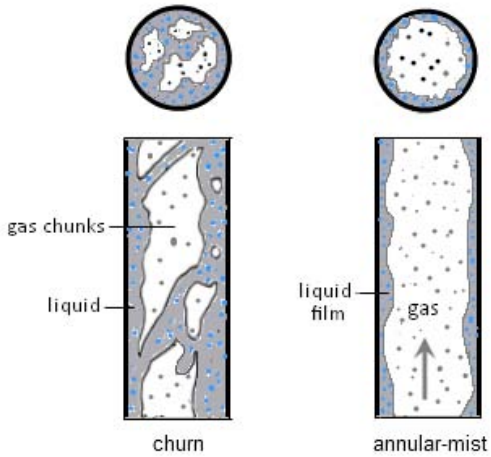

Figure 2: Schematics of vertical three-phase churn and annular-mist flow patterns.

Depending on the flow pattern and water cut, the oil and water liquid phases can flow as stratified or dispersed. The distribution of the two liquid phases and particularly the issue of water wetting the inner pipe wall were the main focus of the present work.

EXPERIMENTAL PROCEDURE

The three-phase flow experiments were conducted in a large-scale inclinable multiphase flow loop. A schematic layout of the flow loop is given in Figure 3. The main flow line of the loop consists of a 30 m long, 0.1 m (4 inch) ID flow line mounted on a steel rig structure. The loop consists of two consecutive legs of PVC pipes connected by a 180-degree bend. This section of the loop is inclinable from 0° (horizontal) to a 90° (vertical). Oil and water liquids are pumped separately from the individual storage tanks into the 0.1 m ID main line by progressive cavity pumps. The gas stream is circulated in the main line by a positive-displacement type gas blower. The fluid mixture flows for approximately 100 pipe diameters in the first upstream leg before reaching the conductivity pins section, used for surface wetting measurement, followed by a transparent PVC pipe section, used for flow pattern visualization. A photo of the test section is shown in Figure 4. Upon exiting the main line, the flow stream is directed to the separation facilities which include a gas-liquid separator, an oil-water separator and a droplet separator. The separated oil and water streams are returned to their respective storage tanks while the dry gas is recirculated by the blower.

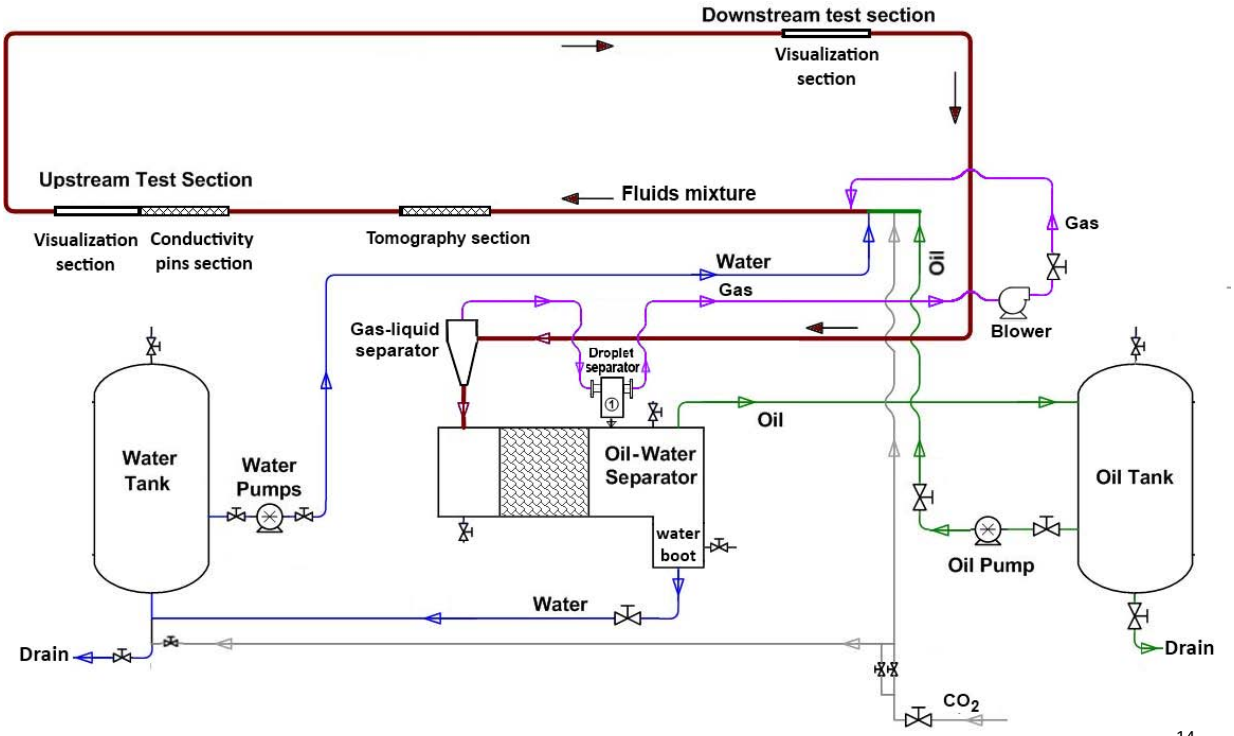

Figure 3: Schematic layout of the inclinable 0.1 m ID flow loop used for gas-oil-water flow.[14]

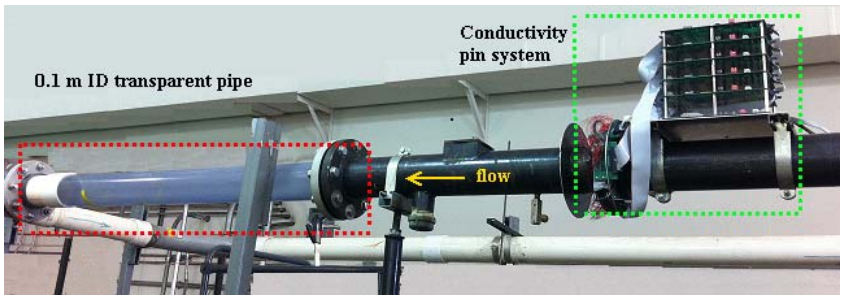

Figure 4: 0.1 m ID transparent pipe and pin test section fitted with conductivity pins.

High Speed Camera

The flow pattern visualization was obtained by use of a high speed video camera (model Vision Research Phantom V12.1*) through a 0.1 m ID transparent PVC pipe. The camera was set up with a framing rate of 6,000 fps in order to capture the fast-motion multiphase fluid flow patterns clearly. During the experiments, the transparent pipe was illuminated with a high intensity light source with a light diffuser placed in between. The light source was positioned behind the transparent pipe such that the illumination through the pipe would be directly opposite the camera lens on the other side of pipe. The camera settings and filming of the video files (in ".cine" format) were controlled through the video software connected to a host computer.

Conductivity Pins

The surface wetting was determined using conductivity pins which were flush mounted on the internal wall of 0.1 m ID test section. Two types of conductivity pins pipe sections were used: one comprised of 93 pins covering one half (180°) of the pipe circumference (Figure 5), named the "180° pins section", and the other comprised of 160 pins covering the entire pipe circumference, named the "360° pins section". The 180° pins section is suited for horizontal flow where water is mainly at the pipe bottom; while the 360° pins section is suited for vertical flow where the water can be anywhere. The design and working principle of the conductivity pins have been discussed elsewhere.[6] Since oil and water are vastly different in electrical conductivity, the pin circuit will display a contrasting voltage drop signal that can distinguish the phase locally wetting the pipe wall as either being water or oil. If a pin is covered by the water phase, the fluid resistance is low, resulting in a low voltage drop V_{in} in the pin circuit, and vice versa for a pin covered by oil. The voltage drop response, V_{in}, can then be compared with a reference voltage V_{ref} in a comparator circuit to produce a two-level signal that can be interpreted as: *water wet* if $V_{in} < V_{ref}$, or *oil wet* if $V_{in} > V_{ref}$. The pin wetting information for the pins section is displayed simultaneously as a pictorial wetting snapshot shown in Figure 5(b), where the solid black circles refer to water wet pins and hollow white circles refer to oil wet pins. Before running the experiments, the test section was thoroughly polished to remove grime on the pins, followed by a continuous 'rinse' with gas-oil slug flow to condition the pins before any measurements were taken.[14]

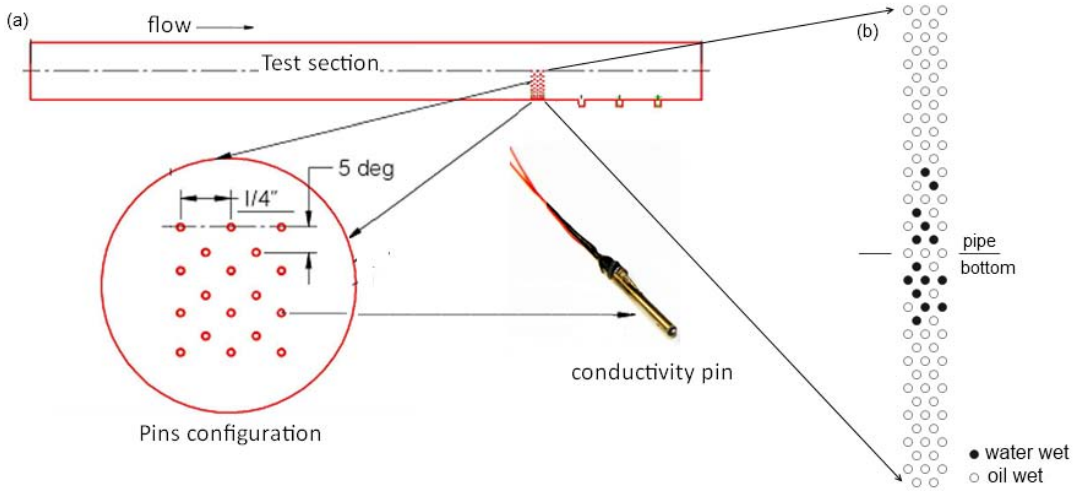

Figure 5: a) Schematic layout showing conductivity pins array flushed mounted on the internal wall of 180° pin section covering the lower half of pipe circumference, (b) Typical wetting pins array snapshot.

* Trade Name

Test Matrix

The flow loop was setup to study the three-phase flow in both horizontal and vertical pipe configurations with varying water cuts. Two types of measurements, a) flow pattern and b) surface wetting were taken for the various flow conditions shown in test matrices in Table 2. For each series of experiments, the test sequence was executed at fixed water cuts by varying the mixture liquid velocity V_m and the superficial gas velocities V_{sg}. The mixture liquid velocity V_m is the sum of superficial oil and water velocities. Once the flow was fully developed, the flow pattern was captured by the high speed video camera through the PVC transparent pipe section. The wetting data were measured by the conductivity pins after consistent wetting behavior was achieved. The test fluids used were light model oil LVT200 (40 °API) as the oil phase, aqueous 1 wt.% NaCl solution saturated with CO_2 and CO_2 as the gas phase. In order to provide better contrast for flow visualization, red food dye (red 44) of 250 ppm concentration was added to the water. The dye did not affect the interfacial tension. The properties of the test fluids are listed in Table 3. The flow loop experiments were performed by first establishing the two-phase oil-water flow at the tested mixture liquid velocity. The gas was then circulated and gradually increased, resulting in transition from one flow pattern to another.

Table 2
Test matrices for horizontal and vertical three-phase flow experiments

Parameter	Value	
Oil phase	LVT200	
Water phase	1 wt.% NaCl aqueous	
Gas phase	CO_2	
Pipe ID (m)	0.1	
Inclination (°)	0° (horizontal)	90° (vertical)
Mixture liquid velocity V_m (m/s)	0.2 – 1.5	0.5 – 1.5
Superficial gas velocity, V_{sg} (m/s)	1 – 45	5 – 45
Water cut (%)	1 – 20	1 – 10

Table 3
Fluids properties used in this work

Parameter	Value @ 25 °C		
	Oil phase	Water phase	Gas phase
Fluid	LVT200	1 wt.% NaCl (aq.)	CO_2
Density (kg/m^3)	823	1000	1.8
Dynamic viscosity (cP)	2.7	1	0.015
Surface tension (mN/m)	28.5	72	-
Oil-water interfacial tension (mN/m)	40.5		N.A.
Water-in-oil contact angle (°)	73		N.A

RESULTS AND DISCUSSION

Horizontal Flow Patterns

The horizontal flow pattern results from the high speed camera are presented in Figure 6 for 1% water cut and in Figure 7 at 20% water cut. For each series of results, the flow patterns are shown in the order of increasing superficial gas velocity V_{sg}, which typically starts from elongated bubble (*EA*), then slug (*SL*), wavy annular (*WA*), and finally annular-mist (*AM*) flows. The global structures for each flow pattern have been described in the previous section. The results here will focus on the distribution of

water in the liquid flow structure. There are two possible types of local distribution of oil and water phases within the liquid flow structure: *separation* and *dispersion.* In *separation,* the water and oil flow as separated phases in the pipe. Here, water is always in contact with the pipe wall. In *dispersion,* the water phase is dispersed as droplets in the continuous oil phase. Depending on the degree of dispersion and amount of water, the water droplets may or may not contact the pipe wall intermittently.

As shown in Figure 6 for the horizontal flow at 1% water cut, the water droplets are rather large (3 mm to 6 mm) and concentrate in the lower pipe section in low gas velocities but become smaller and more dispersed as the gas velocity increases. By increasing to water cut of 20% in Figure 7, the lower half of the pipe shows an accumulation of a thick layer of water phase in *EB* and *SL* flows. The water layer consists of a continuous film and densely packed water droplets that moves rather slowly. As the gas velocity increases, the water becomes highly mixed with oil and gas phases in the flow. In *WA* and *AM* flows, the flow becomes more opaque due to the increased gas entrainment within the fluid mixture. Though water is hardly discernible at high gas velocities, the water is mostly in a dispersion state because of the intense turbulence in the flow. The fast moving gas tends to occupy the pipe core and displaces the liquid phases towards the pipe circumference where the visibility is poor. Hence, the interaction of the liquid film with the pipe wall can only be determined by the use of conductivity pins, which would detect which local liquid phase comes in contact with the pipe wall surface.

All the experimental flow data points from the experiments were entered into the flow pattern maps as shown in Figure 8(a) for 1% water cut and Figure 8(b) for 20% water cut. The transition lines separating the flow patterns are also included in the maps. Upon comparison, the change of water cut from 1% to 20% has little influence on the transitions for global gas-liquid flow structures. The difference is in the local distribution of the water phase within the oil-water liquid phase, where water is more easily entrained in low water cut than in high water cut with the other conditions being the same.

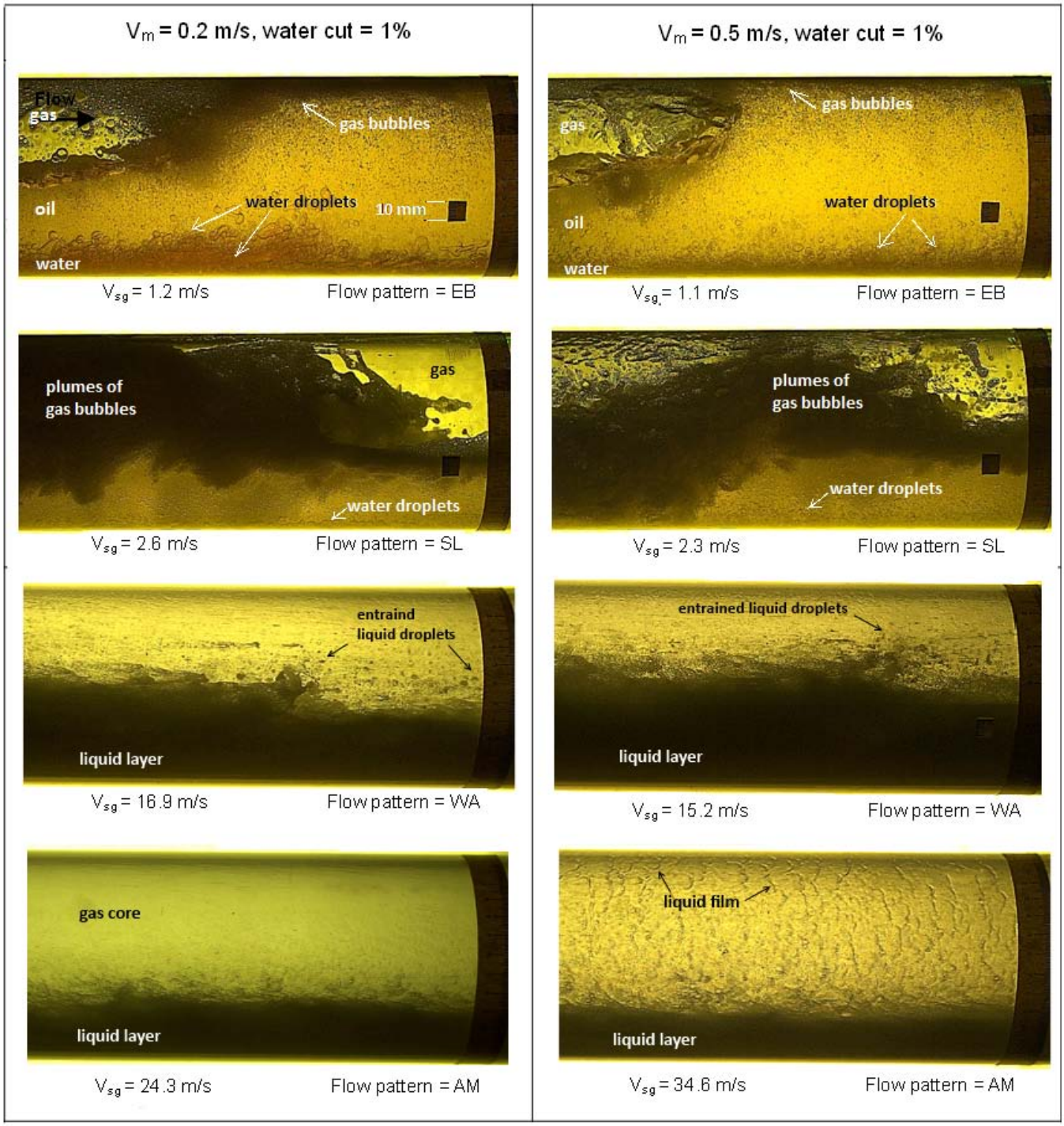

Figure 6: Images of flow patterns at V_m = 0.2 – 0.5 m/s, 1% water cut for CO_2–LVT200–water system.

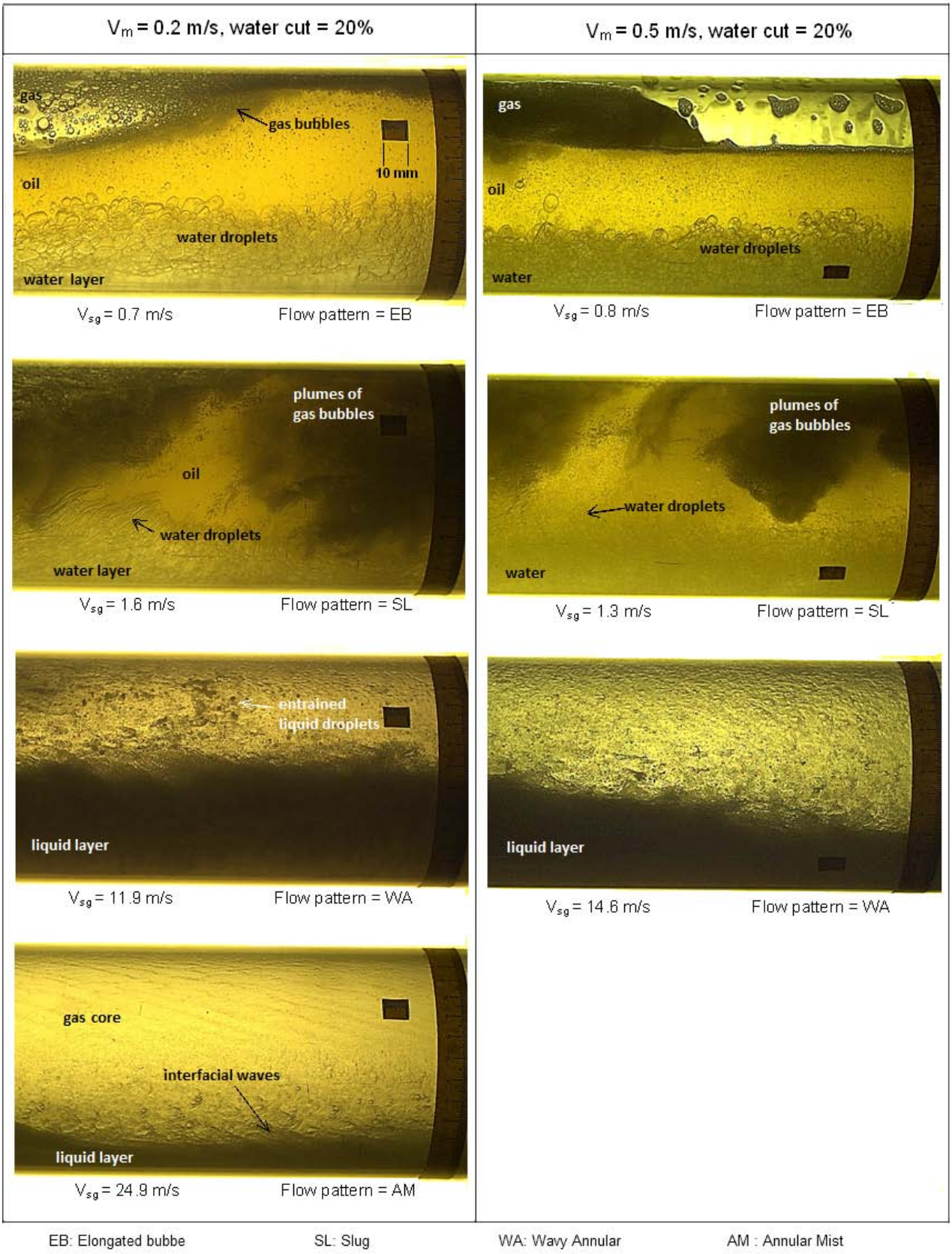

Figure 7: Images of flow patterns at V_m = 0.2 – 0.5 m/s, 20% water cut for CO_2–LVT200–water system.

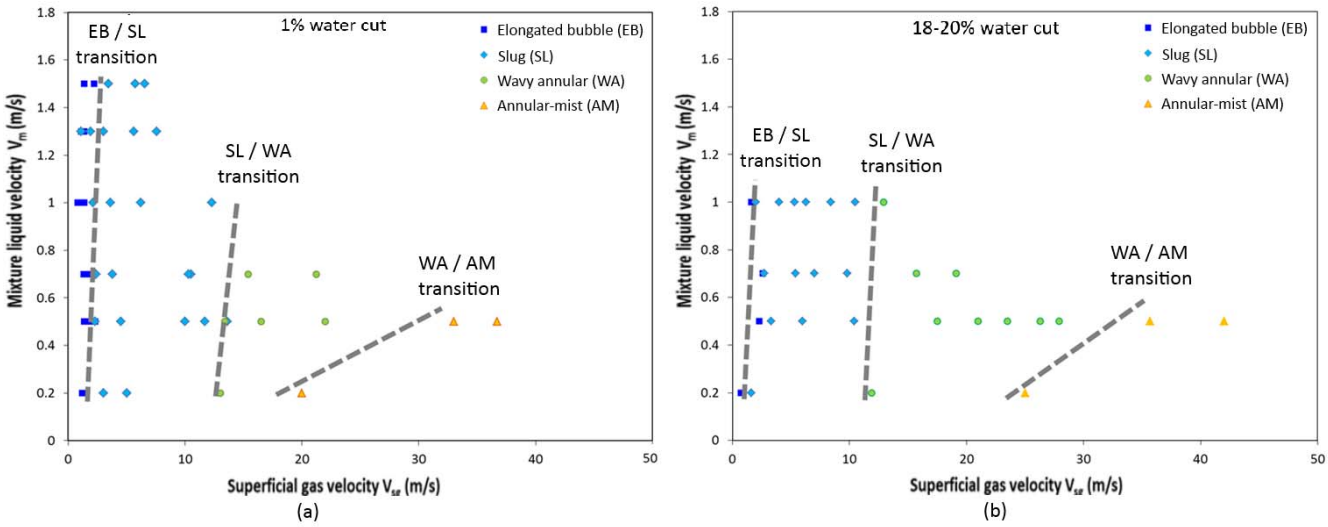

Figure 8: Flow pattern map for horizontal CO_2–LVT200–water system at: (a) 1%, (b) 18%-20% water cut.

Surface Wetting in Horizontal Flow

Four types of surface wetting regimes can be identified from the conductivity pin wetting analyses:[14]

Stable water wet	:	some pins are water wet and stay water wet.
Unstable water wet	:	more than 3% of the pins stay water wet, some pins change intermittently between oil wet and water wet.
Unstable oil wet	:	not more than 3% of the pins stay water wet, some pins change intermittently between oil wet and water wet.
Stable oil wet	:	all pins are oil wet.

It should be noted that both *unstable water wet* and *unstable oil wet* display intermittent behavior but with different degree of wetting intermittency. The former is predominantly water wet with some pins switching intermittently between oil/water wet, while the latter is mostly oil wet with few intermittent pins. From the corrosion standpoint, the *water wetting* condition includes the stable and unstable water wet behaviors where the corrosion is likely to occur, while the *oil wetting* condition encompasses the stable and unstable oil wet behaviors where the corrosion is unlikely or minimal. The pin system is built with redundancy with many pins on the wall. It was empirically established that 3% threshold was appropriate to minimize the effect of non-responsive pins or other outliers.[7]

Figure 9(a) shows the surface wetting map for 1% water cut in horizontal gas-oil-water flow. Each data point represents one of the four wetting regimes as stated above. A wetting transition line is drawn on the map to represent the observed wetting behavior change from *water wetting* to *oil wetting*. The results showed that the water wetting prevailed when the mixture liquid velocity was low ($V_m \leq 1$ m/s) and the gas velocity was at the lowest ($V_{sg} \leq 1$ m/s), with the flow patterns identified as *EB* flow. As evidenced from the flow visualization results in Figure 6, the water wetting was caused by the water droplets that dropped out and agglomerated in the bottom wall around 4 to 8 o'clock pipe position. As V_{sg} increased beyond 1 m/s, the flow patterns began transition to *SL*, *WA* and *AM* flows, while the *water wetting* occurrence began to diminish at the pipe bottom. Few instances of intermittent wetting occurred at the side (3 o'clock) and bottom of the pipe wall, resulting in *unstable oil wet* and *stable oil wet* conditions. The behavior was in accordance with the vigorous mixing actions of the turbulent flow that can disperse and suspend the small amount of water phase. The wetting results at 1% water cut indicated that *oil wetting* can be achieved with increasing gas velocity, especially in *WA* and *AM* flows.

Figure 9(b) show the surface wetting map for 18% to 20% water cut in horizontal gas-oil-water flow. The wetting results were similar to the 10% water cut (not shown here), where *stable water wet*

condition was observed at pipe bottom when the gas velocity was low (V_{sg} < 3 m/s), and changed to *unstable water wet* condition with increasing gas velocities, accompanied by the transitions of flow patterns from *EB* to *SL*, *WA* and *AM* flows. At such high water cut, the water phase was not fully entrained by the turbulent flow. In *WA* and *AM* flows, though water was not clearly discernible from the flow visualization in Figure 7, it appeared that fast flowing gas pushed the liquid phase to the wall which greatly enhanced the possibility of water wetting the wall surface.

Figure 10(a) and (b) present the wetting snapshots depicting the changes of surface wetting with increasing V_{sg} at liquid velocity V_m = 0.5 m/s for 1% and 20% water cuts, respectively. At 1% water cut, the water wetting behavior diminished with increasing V_{sg}. Contrarily, the water wetting intensity did not lessen with increasing V_{sg} at 20% water cut .The water wetted area was seen to concentrate in the lower section of the pipe in low V_{sg} and began to spread up to the pipe sides as V_{sg} increased. At high V_{sg} = 45 m/s in *AM* flow, the lower half of the pipe circumference was unstably wetted by water.

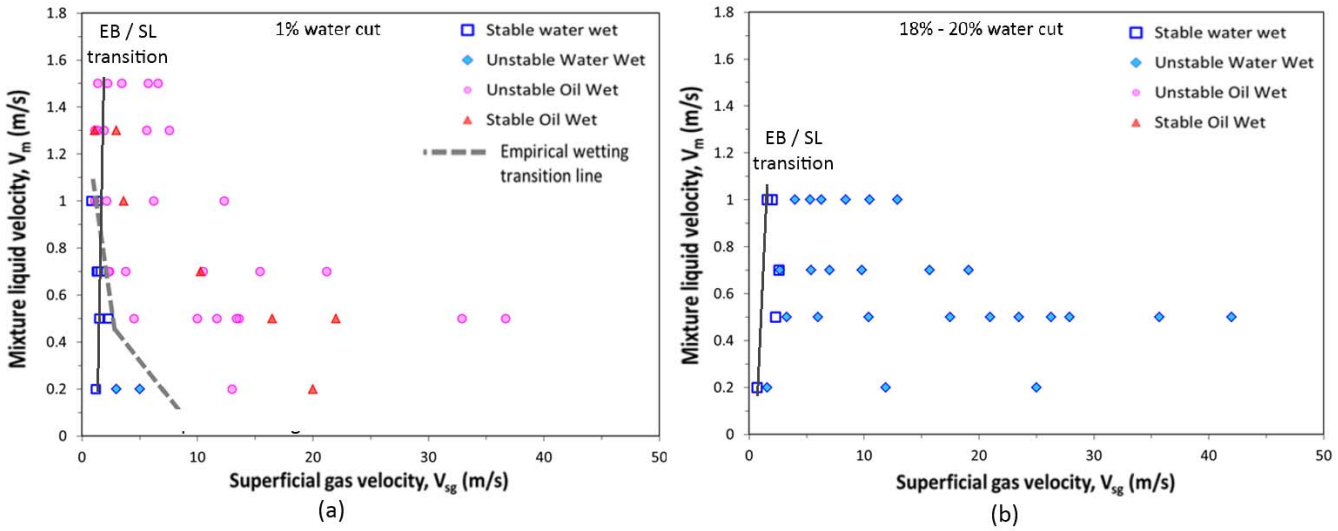

Figure 9: Surface wetting map for horizontal CO_2–LVT200–water system at: (a) 1%, (b) 18%–20% water cut.

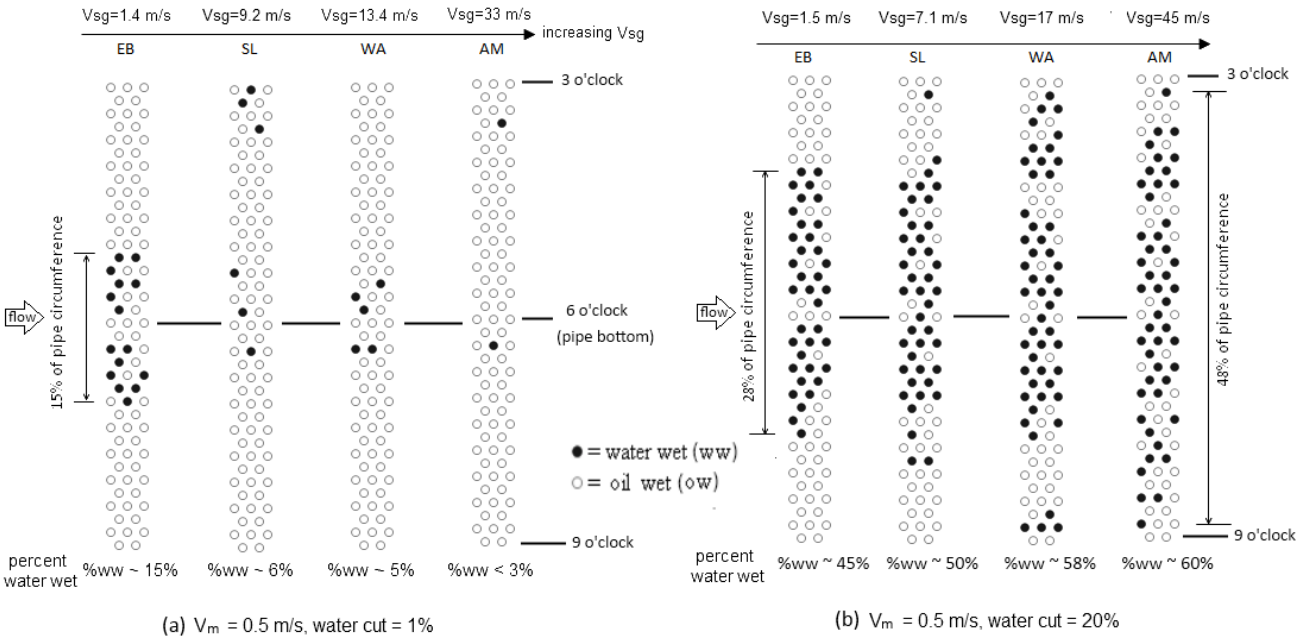

Figure 10: Wetting snapshots for horizontal flow at increasing gas velocities. Flow conditions: V_m = 0.5 m/s (a) 1% water cut (b) 20% water cut.

Vertical Flow Patterns

The flow visualization from the high speed video camera showed that *churn* flow (Figure 11) prevailed in the lower range of V_{sg} between 6 m/s to 22 m/s. Ohnuki & Akimoto also reported that churn flow was dominant in a large diameter vertical pipe under the conditions where slugs would normally occur in a small diameter pipe.[19] The sequential evolution of churn flow is presented in Figure 11, showing the characteristic oscillatory fluid motion. Upon increasing the gas velocities beyond 25 m/s, the intermittent flow showed gradual transition to annular-mist flow, characterized by the presence of liquid film moving upward on the wall and gaseous phase in the pipe core (Figure 12). The flow appearance was similar for all tested water cuts from 1% to 20%. It should be stressed that the transition between the flow patterns was gradual without a distinctive transition boundary. The benefit of flow visualization became somewhat limited due to the increased opaqueness of the fluid mixtures as the gas velocity was increased. The experimental data points were plotted in flow pattern maps as shown in Figure 13(a) for 1% water cut and Figure 13(b) for 20% water cut. Upon comparison between the low and high water cuts, the flow shows quite similar conditions for churn to annular-mist (*INT/AM)* transition.

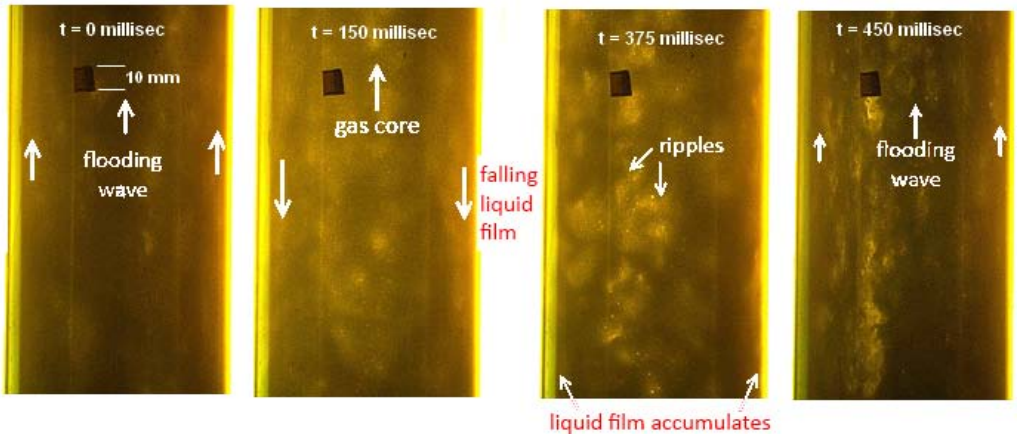

Figure 11: Sequential images for the evolution of churn flow at V_m = 0.5 m/s, 10% water cut, V_{sg} = 22 m/s.

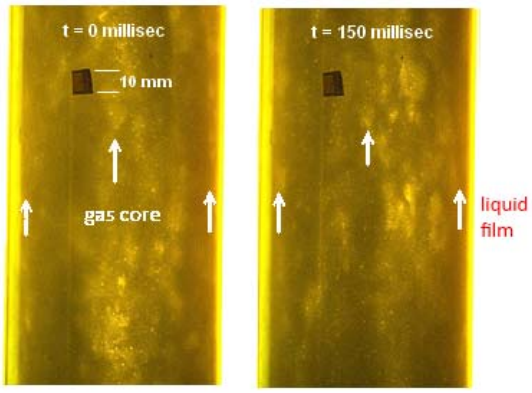

Figure 12: Sequential images for annular-mist flow at V_m = 0.5 m/s, 10% water cut, V_{sg} = 47 m/s.

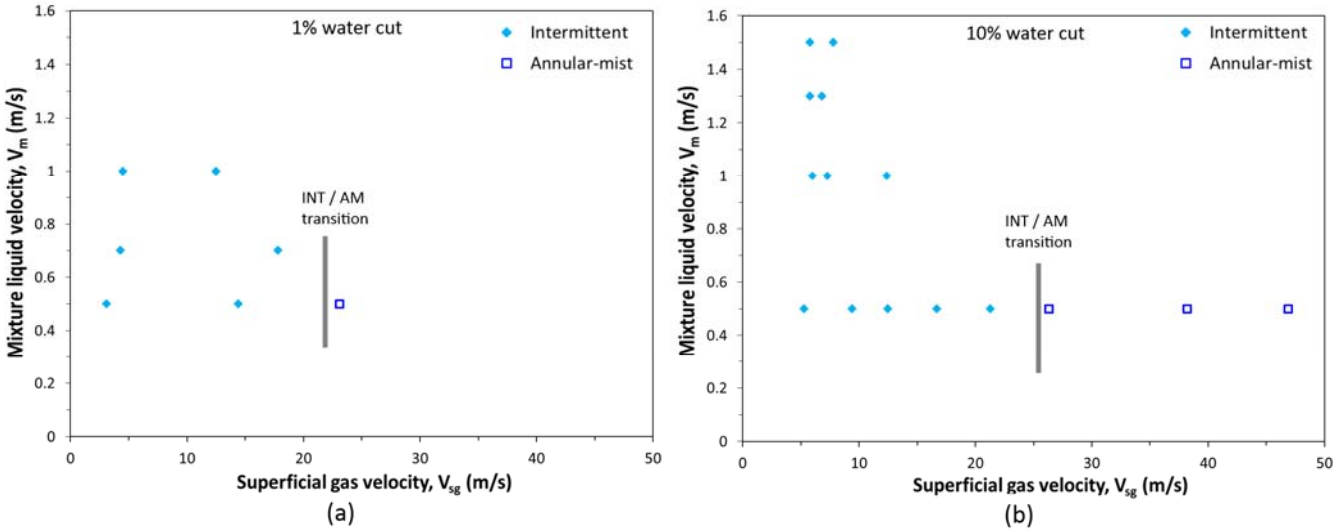

Figure 13: Flow pattern map for vertical CO_2–LVT200–water flow at: (a) 1% water cut, (b) 10% water cut.

Surface Wetting in Vertical Flow

Figure 14(a) shows the surface wetting map for the vertical gas-oil-water flow at 1% water cut. The corresponding flow patterns can be cross-referenced with Figure 13(a) which are either churn flow or annular-mist flow. The overall surface wetting results were indicative of *unstable oil wet* where the majority of pin area appeared to be oil wet, with 2 to 4 pins switching between oil wet/water wet at random circumferential locations as shown in Figure 15(a). *Unstable oil wet* behavior prevailed even when the liquid velocity and/or gas velocity was increased. These wetting results implied that the entrained water droplets occasionally wet the pipe wall. A continuous water layer was not observed from the flow visualization and the flow appeared to be highly mixed with oil, water and gas phases. The fluid mixtures were frequently churned and transversely displaced adjacent to the wall when the gas blew through the pipe core, more so at higher gas velocity. Figure 14(b) shows the surface wetting map for the vertical gas-oil-water flow at 10% water cut where *unstable water wetting* prevailed for all tested flow conditions. The wetting results were similar for the 5% water cut (not shown here). Upon examining the wetting snapshots, the pin area wetted by water spans almost the entire pipe circumference and the wetting intensity was not lessened by the increase of liquid and/or gas velocities. It appeared that with water cut ≥5%, the likelihood of water wetting the pipe wall was greatly enhanced.

Figure 15(a) and (b) present the wetting intensity snapshots depicting the changes of surface wetting with increasing gas velocity V_{sg} at V_m = 0.5 m/s for 1% and 10% water cuts, respectively. The observed flow pattern in both cases was churn flow. At 1% water cut, *unstable oil wet* prevailed and stable oil wet condition was not achieved. Approximately 3% of the measurement area was still intermittently and randomly wetted by the water phase as detected by the conductivity pins. At 10% water cut, almost the entire span of pipe circumference was randomly and intermittently wetted by water. The increase of gas velocity could not lessen the extent of unstable water wetting.

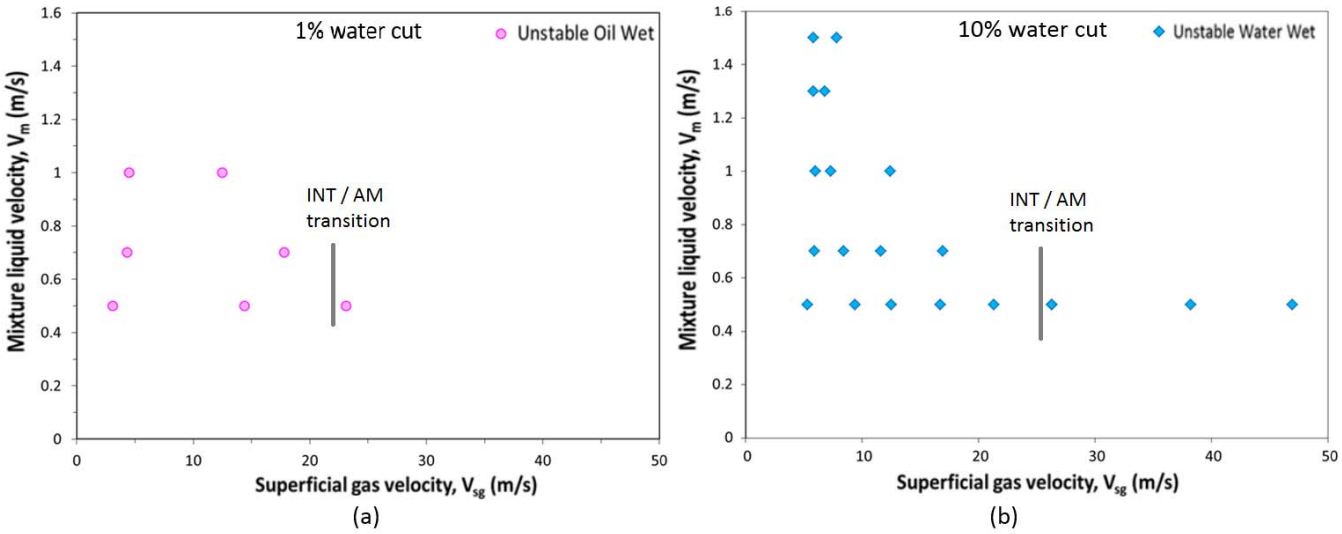

Figure 14: Surface wetting results for vertical CO_2–LVT200–water flow at: (a) 1% water cut, (b) 10% water cut

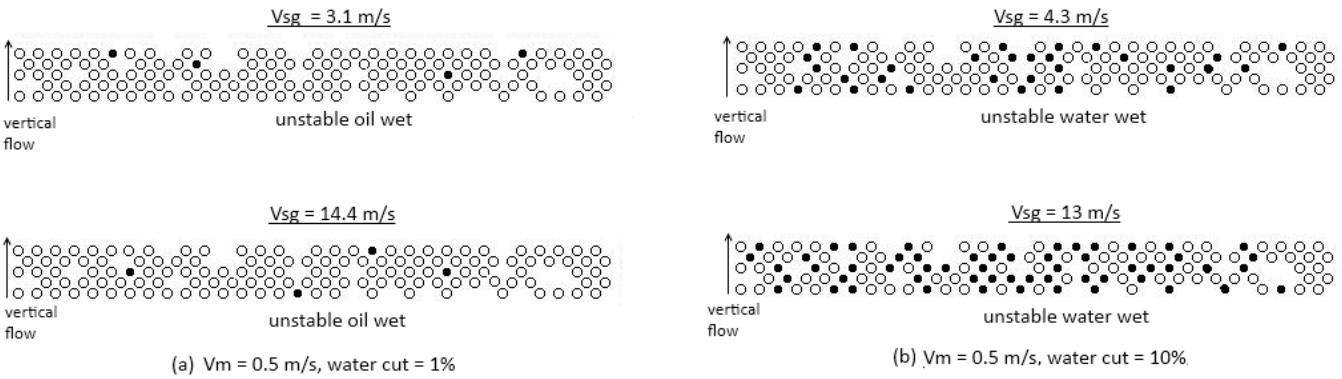

Figure 15: Wetting snapshots for vertical flow at different superficial gas velocities. Vertical flow condition: V_m = 0.5 m/s at: (a) 1% water cut, (b) 10% water cut.

CONCLUSIONS

- The three-phase flow patterns can be categorized according to the global flow structure seen in gas-liquid flow. Elongated bubble, slug, wavy annular and annular-mist flow patterns were observed in horizontal flow. Churn and annular-mist flow patterns were observed in vertical upward flow.
- The local water distribution was found to dynamically vary according to different locations in the flow structure.
- In horizontal flow with low water cuts of 1%, water separated out at low gas velocity, leading to water wetting at the pipe bottom. At higher gas velocity, where wavy annular or annular-mist flows were dominant, water was mostly dispersed, reducing the extent of water wetting and showing unstable oil wetting.
- At high water cut 10%-20%, the water wetting behavior prevailed in the lower half of the pipe. The increase in gas velocity did not reduce the extent of water wetting. The water wetted area was seen to spread up to both sides of the pipe in response to the flow regime transition.

- In vertical flow, unstable oil wetting was observed at 1% water cut in churn and annular-mist flows. The behavior changed to predominantly water wetting at higher water cut above 5%. The water wetted area was extended to the entire pipe circumference.
- A correlation could be established between the three-phase flow patterns and the water wetting behavior. The pipe orientation (horizontal vs. vertical) and water cut influences the water distribution in different flow patterns, hence affecting the water wetting.

ACKNOWLEDGEMENTS

The authors wish to thank the financial support and technical directions from the sponsoring companies of the water wetting JIP: BP, ConocoPhilips, ExxonMobil, Petrobras, Saudi Aramco, and Total. Support from Universiti Teknologi Petronas is appreciated

REFERENCES

1. A. Valle and O. H. Utvik, “Pressure drop, flow pattern and slip for two phase crude oil/water flow: Experiments and model predictions,” in Int. Symposium on Liquid-Liquid Two Phase Flow and Transport Phenomena (Antalya, Turkey: 1997).
2. P. Angeli and G. F. Hewitt, “Flow structure in horizontal oil-water flow,” *Int. J. Multiphase Flow*, vol. 26, no. 7 (2000): pp. 1117–1140.
3. M. Vielma, S. Atmaca, C. Sarica, and H.-Q. Zhang, “Characterization of Oil/Water Flows in Horizontal Pipes,” *SPE Projects, Facil. & Const.*, vol. 3, no. 4 (Dec. 2008): pp. 3133–3143.
4. J. Cai, S. Nesic, C. Li, X. Tang, F. Ayello, C. Ivan, T. Cruz, and J. Al-Khamis, “Experimental studies of water wetting in large-diameter horizontal oil/water pipe flows,” SPE Annual Technical Conference and Exhibition (Richardson, TX: SPE 2005), pp. 719–731.
5. C. Li, X. Tang, F. Ayello, J. Cai, S. Nesic, C. I. Cruz, and J. Al-Khamis, “Experimental study on water wetting and CO2 corrosion in oil-water two-phase flow,” CORROSION/2006, paper no. 06595 (Houston, TX: NACE, 2006).
6. J. Cai, C. Li, X. Tang, F. Ayello, S. Richter, and S. Nesic, “Experimental study of water wetting in oil-water two phase flow-Horizontal flow of model oil,” *Chem. Eng. Sc.*, vol. 73 (2012): pp. 334–344.
7. K. E. Kee, S. Richter, M. Babic, and S. Nešić, “Flow patterns and water wetting in oil-water two-phase flow - A flow loop study,” in CORROSION/2014, paper no. 4068, 2014, pp. 1–15 (Houston, TX: NACE, 2006).
8. J. Trallero, C. Sarica, and J. Brill, “A study of oil-water flow patterns in horizontal pipes*,” SPE Prod. Facil.,* vol. 12, no. 3 (1997): pp. 165–172.
9. J. Flores, X. Chen, C. Sarica, and J. Brill, “Characterization of Oil–Water Flow Patterns in Vertical and Deviated Wells,” *SPE Prod. Facil.*, vol. 14, no. 2 (1999): pp. 102–109.
10. H. Shi, J. Cai, and W. P. Jepson, “Oil-water two-phase flows in large-diameter pipelines,” *J. Energy Resources Technol.*, Trans. ASME, vol. 123, no.2–4 (2001): pp. 270–276.
11. M. Açikgöz, F. França, and R. T. Lahey, “An experimental study of three-phase flow regimes,” *Int. J. Multiphase Flow*, vol. 18, no. 3 (1992): pp. 327–336.
12. A. H. Lee, “A study of flow regime transitions for oil-water-gas mixtures in large diameter horizontal pipelines,” (M.S. thesis, Ohio University, Athens, 1993).

13. C. Keskin, H. Zhang, and C. Sarica, “Identification and Classification of New Three-Phase Gas/Oil/Water Flow Patterns,” in Proc. of SPE Annual Tech. Conf. & Exh., paper no. 110221, (SPE 2007), pp. 1–13.
14. K. E. Kee, “A study of flow patterns and surface wetting in gas-oil-water flow,” (Ph.D. dissertation, Ohio University, Athens, OH, 2014).
15. A. Dukler and M. Hubbard, “A model for gas-liquid slug flow in horizontal and near horizontal tubes,” *Ind. & Eng. Chem. Fundamentals*, vol. 14, no. 4 (1975): pp. 337–347.
16. O. Shoham, *Mechanistic modeling of gas-liquid two-phase flow in pipes*. (Richardson, TX: Society of Petroleum Engineers, 2006).
17. T. W. F. Russell and D. E. Lamb, “Flow mechanism of two-phase annular flow,” *Can. J. Chem. Eng.*, vol. 43, no. 5 (1965): pp. 237–245.
18. S. Jayanti and G. F. Hewitt, “Prediction of the slug-to-churn flow transition in vertical two-phase flow,” *Int. J. Multiphase Flow*, vol. 18, no. 6 (1992): pp. 847–860.
19. A. Ohnuki and H. Akinomoto, “Experimental study on transition of flow pattern and phase distribution in upward air-water two-phase flow along a large vertical pipe,” *Int. J. Multiphase Flow*, vol. 28, no. 3, pp. 367-386.